Experimental investigation of a plane wall jet : application to vertical refrigerated display cabinet

A. Kaffel, J. Moureh, J.L. Harion, S. Russeil

EXPERIMENTAL INVESTIGATION OF PLANE WALL JET: APPLICATION TO VERTICAL REFRIGERATED DISPLAY CABINET

*A. KAFFEL [(a), (b), (c)], J. MOUREH [(a)], J-L. HARION [(b), (c)], S. RUSSEIL [(b), (c)]

[(a)] Refrigerating Process Engineering Unit, Irstea Antony, 1 rue Pierre-Gilles de Gennes - CS10030 92761 Antony Cedex, France

[(b)] Univ Lille Nord de France, F-59000 Lille, France

[(c)] Mines Douai, EI, F-59500 Douai, France

*(Corresponding author: Ahmed.kaffel@irstea.fr)

ABSTRACT

This paper examines the aerodynamic behavior of a plane wall jet exposed to a lateral perturbing flow. The key benefit of this investigation is to bring new knowledge which helps in designing better air curtains operating in disturbed environments. For this purpose, a new experimental setup is achieved which consists of one-fifth scale model of a real refrigerated display cabinet (RDC) enabling the control of the ambiance, the cavity (zero-depth in the present paper) and the jet. PIV measurements of the flow development characteristics such as mean velocity, spread and decay rate have been performed. Results show the role of the perturbing lateral flow in the reduction of engulfed ambient air into the air curtain. Instantaneous PIV results show that the perturbed flow strongly affect the formation, development process and frequency shedding of Kelvin-Helmholtz vortices in the shear layer in the near field region.

NOMENCLATURE

x, y, z	Streamwise, wall-normal and span-wise directions in Cartesian coordinates	(m)
$y_{0.5}$	Lateral distance at which $U = U_m/2$	(m)
e	Nozzle width	(m)
ν	Kinematic viscosity	(m^2s^{-1})
U_0	Nozzle exit velocity	(ms^{-1})
U	Local velocity	(ms^{-1})
U_m	Local maximum velocity	(ms^{-1})
U_{lf}	Lateral flow velocity	(ms^{-1})
f	Vortex shedding frequency	(s^{-1})
St_e	Strouhal number $St_e = fe/U_0$	(–)
Re	Reynolds number	(–)

ACRONYMS

RDC	Refrigerated Display Cabinet
ELS	External Lateral Stream
PIV	Particle Image Velocimetry

1. INTRODUCTION

The use of air curtains is of major importance in several fields such as air conditioned areas, dust and humidity control, commercial entrances, etc. Air curtains are also used for cold storage purposes. In our case we are interested in refrigerated display cabinets (RDC). Airflow patterns developed by air curtains devices are very important to keep food at prescribed regular temperatures, while allowing an energy-saved control

and an open access for customers. Due to their design, RDC are very sensitive to ambient conditions and they are considered as the weakest link of the cold chain. A fully loaded RDC can reasonably be simplified to an academic configuration of a plane wall jet. Previous studies only assessed the efficiency of the RDC in quiescent ambient conditions. However, these facilities generally used in open spaces like supermarkets, are very sensitive to external perturbations generated by human activities such as pressure difference due to door opening, parasitic air draughts, action of air conditioning system, etc. Such perturbations strongly affect the stability, the air tightness, the transfer mechanisms and therefore the efficiency of air curtain due to a lack of confinement which leads to an increase of energy consumption (Gaspar et *al.*, 2011). This study is a first step in a research activity aiming to investigate the aerodynamic behavior in a RDC subjected to external perturbation. It focuses on the case of a wall jet which represents an idealized configuration of an air curtain device operating in a fully loaded RDC. Such hypothesis also allows performing more fundamental study on the physics of an air wall jet, while avoiding more case-specific geometries used by many authors (Cortella, 2002, Laguerre *et al*., 2012). According to typical RDC dimensions, the corresponding air curtain lengths are about ten jet widths. Therefore, RDC air curtain flows reside in the transitional flow regime (Field and Loth, 2006), which is not yet well understood. In addition to the RDC case, studying transitional disturbed wall jets can provide further understanding of the fundamental nature of the flow, leading to improvements in various practical applications where wall jets evolve in non-quiescent ambience.

There are two distinct layers in the wall jet configuration as first proposed by Glauert (1956): an inner layer located between the wall and the maximum in the velocity profile, that behaves like a viscous boundary layer; and an outer free shear layer where the turbulence of the main flow plays an important role, that is subjected to the inviscid Kelvin-Helmholtz instability and the development of large scale vortices. The interaction between large scale structures from the outer layer and inner layer influences the laminar-to-turbulence transition.The first turbulence measurements of the wall jet were conducted by Bradshaw and Gee (1960). They found that the shear stress tensor value doesn't vanish at the position of maximum streamwise velocity which proves the existence of interaction between inner and outer layers. One of the earliest experimental studies on transitional plane wall jets was conducted by Bajura and Catalano (1975). They found that the Kelvin-Helmholtz instability of the free shear layer plays a key role in the transition of the wall jet. Hsiao and Sheu (1996) carried out an experimental study using hot wire anemometry and flow visualization (300< Re <30.000).They found that the growth of vortices originating from small perturbations in the outer shear layer serves as a trigger for the transition process.

Field and Loth (2006) studied the air curtain modeled as a negatively–buoyant wall jet. They used particle image velocimetry (PIV) visualization as an experimental tool to define the air curtain vortex structures, they found that a variety of eddy engulfing structures are responsible of the entrainment of ambient air into the jet, this process which arises from shear layer interaction is enhanced by high initial turbulence level in the curtain jet. The instantaneous velocity measurements through PIV technique conducted by Cao et al. (2010) in the near wall region revealed the existence of the double row vortex pairing structure where small scale vortex has been detected in the near wall region. Recently, Hoof et al. (2012) have conducted an experimental study via PIV technique of the transitional plane wall jet (Reynolds number ranging from 800 to 2500) in a confined enclosure. They used Q criterion (a scalar used to visualize vortex regions, they are detected where $Q > 0$ which means that the vorticity magnitude dominates the rate of strain, see Hunt et al., 1988)) to extract vortical structures in the outer region of the wall jet, They noted that eddy structures number increases with Reynolds number. Hence, the Strouhal number increases with higher Reynolds number.

The aim of the present work is to experimentally investigate the aerodynamic behavior of a wall jet subjected to external lateral stream by means of PIV measurement technique. This study will be performed on a reduced-scale model representing a generic configuration of a RDC by focusing on the near field region (x/e which denotes the ratio between vertical height and jet width < 10), where strong interactions are expected between the jet core, wall boundary and external lateral stream.

2. EXPERIMENTAL SETUP AND PROCEDURE

The experimental setup shown in (Figure1.A) is a scaled-down (1:5) model of a vertical open refrigerated display cabinet (RDC). It represents an air curtain confining a cavity subjected to an external flow under

isothermal conditions. Using scaled-down model as generic configuration of a RDC is very useful to characterize the fundamental nature of flow field while eliminating case-specific issues particular to each manufacturer. The key benefits and originality of this facility is that it allows us to investigate the behavior and stability of the wall jet subject to an external lateral stream (ELS) with the control of different parameters related to the jet (different Reynolds number), the ELS (different velocities) and the cavity (various depths). The cavity is of 40 cm height and 50 cm width with an adjustable back wall to obtain different depths ranging from 15 cm which corresponds to an air curtain confining a cavity to 0 cm representing a wall jet which corresponds to a fully stocked RDC. In this paper only the configuration of the wall jet is considered. The origin of the coordinate is fixed on the wall at the mid-plane of the nozzle. A definition schematic and measurement configuration of the facility are shown in (Figure1.B). Cartesian coordinates are used, x axis for streamwise direction, y axis for lateral or wall-normal direction and the third z axis for span-wise evolution. Data were acquired in the turbulent regime at Reynolds number of about 8000 (see eq. (1), the slot exit (e) is equal to 4 cm). Measurements have been carried out using a high speed 2D2C PIV system which consists of a double pulsed (10mJ/pulse) Nd:YLF laser emitting light of 527 nm wavelength, a high speed CMOS Photron camera for flow field imaging of 1024×1024 pix^2 resolution with an objective Nikon (50 mm). In all measurement cases 2500 pairs of images are used to provide a good accuracy and statistical convergence of mean and turbulent quantities, convergence of turbulent statistics of higher order are also fairly attained. The whole flow field has been covered by the combination of three fields of view of 1024×512 pixels. Measurements in the downstream locations cover the region between x/e = 2 and x/e = 9. Experimental parameters are summarized in the table below.

$$\mathrm{Re} = \frac{U_0 . e}{\nu} \qquad (1)$$

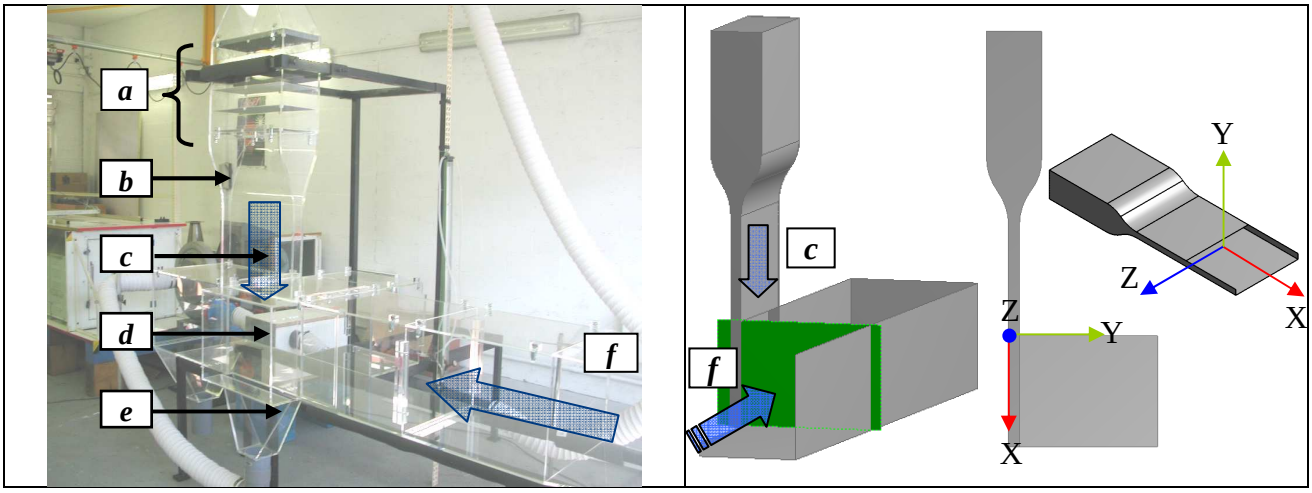

Figure 1. A) Experimental scaled-down test facility of a refrigerated display cabinet (left-hand side) a) settling chamber, b) smooth contraction nozzle, c) air curtain, d) cavity (wall), e) exit of the recycled jet, f) external lateral stream (ELS); B) Measurement plane and coordinates (right-hand side)

Table1.PIV parameters

Frequency	200 Hz
Pulse delay between two laser pulses	900 µs
Field of view	1024×512 pixels
Velocity at the nozzle exit	3 ms^{-1} (Re ≈ 8000), (ν = 15.6 x 10^{-6} at 20°C)
Perturbing velocities	0 ms^{-1} (unperturbed), 0.2 ms^{-1}, 0.5 ms^{-1}, 1 ms^{-1}
Acquisition plane	z = 20 cm

3. PIV VISUALIZATION OF THE UNPERTURBED WALL JET

Figure 2 shows the onset and development of initial eddies of Kelvin-Helmholtz (K-H) type. The roll-up and pairing process of the K-H instability plays a key role in the growth of the shear mixing layer. The effect of lateral perturbation on this process will be shown later.

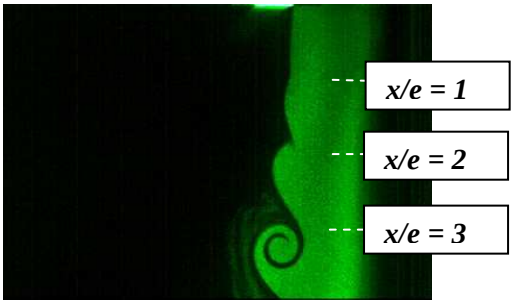

Figure 2 Instantaneous PIV visualisation of Kelvin-Helmholtz instability

4. RESULTS OF THE WALL JET SUBJECT TO THE ELS

4.1. Dimensional profiles of the wall jet subject to ELS of 1ms^{-1}

Figure 3 shows dimensional streamwise velocity profiles of the unperturbed jet (left hand side) and the perturbed jet at 1ms^{-1} (right hand side) at axial positions ranging from x/e = 2 to x/e = 9. A common characteristic of the wall jet is the broadening of the velocity profile at the free shear layer due to the entrainment of the ambient air. This enlargement of the mixing layer is accompanied by an increase of the boundary layer which continues to grow as a result of the friction at the wall. As it can be noticed the velocity profiles exhibits negative values in the case of the perturbed jet. This is due to the presence of a recirculation loop between the two axial positions x/e = 2 and x/e = 5. The lateral flow also tends to move the inflection point closer to the wall.

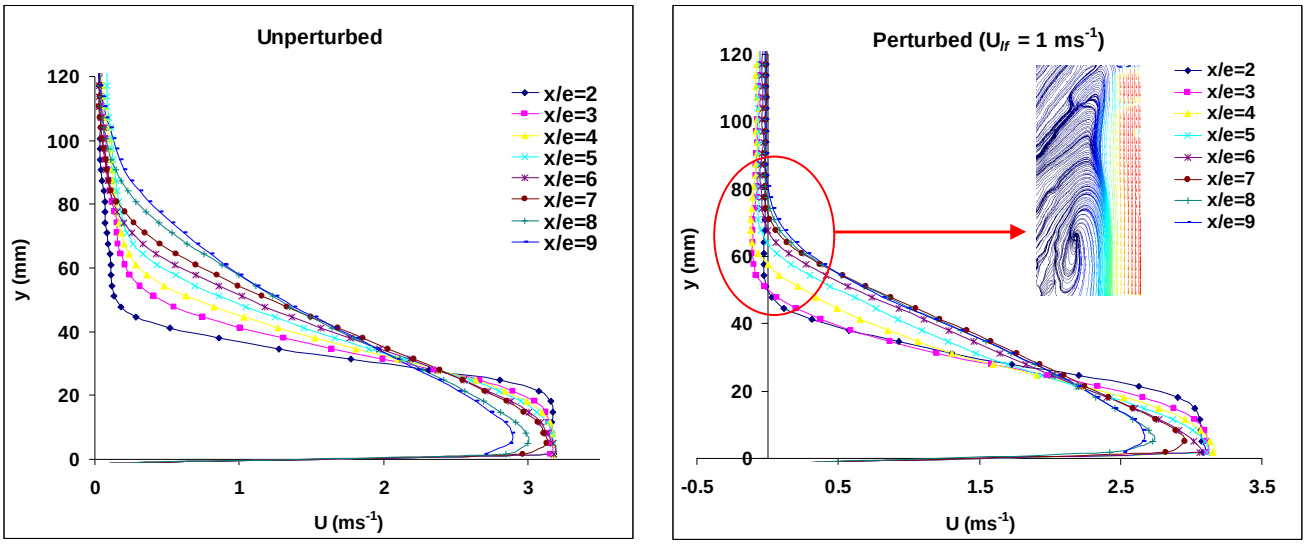

Figure 3 Dimensional profiles of the unperturbed jet (left hand side) and the perturbed jet at 1 ms^{-1} (right hand side)

4.2 Velocity fields and streamlines

Figure 4 illustrates the velocity field distribution and streamlines of the unperturbed and perturbed jet at velocity speed of 0.5 ms^{-1} and 1 ms^{-1}. The whole air curtain is reconstructed from three PIV measurement zones as it has been mentioned earlier. As the jet moves downstream, its mass flow rate increases by entrainment mechanisms from the outer layer. At the return duct located at x/e = 10, the global flow rate

exceeds the recirculated part. Therefore, the jet splits into two different air flow components. The main part of the jet is drawn into the return grill while the non sucked outer part of the air curtain is spilled back into the channel in order to balance the quantity of air that was entrained by the wall jet. The streamlines created by jet entrainment in the upstream part of the jet and those created by the spilling back near the bottom form a global weak two dimensional recirculation which covers the whole channel boundaries as it can be shown in (Figure 4.a). Once the perturbation is introduced at a speed of 0.5 ms-1, the air curtain begins to roll up at the lower part of the channel. Further increase of the perturbation rate at 1ms-1 creates a recirculation loop situated between x/e = 2 and x/e = 5 which also extends over the entire jet as already mentioned in the previous paragraph. Affected by the ELS which come shearing the air curtain, the thickness of the mixing layer decreases and the entrainment of the ambient air is reduced.

4. 3 Decay rate of the maximum streamwise velocity

Figure 5 shows a higher decay rate of the perturbed wall jet determined by plotting U_m/U_0 as a function of x/e. The potential core vary from x/e = 6.7 in the case of the unperturbed jet to about 6.1 when the jet is perturbed at 1 ms^{-1}. Rajaratnam (1976) reported a value of 6.5 in the case of a plane wall jet in a non-recycled quiescent ambient. The perturbed jet is characterized by lower expansion. This suggests that eddies are forced by the lateral perturbing jet to penetrate faster and to consume the potential core leading to an increase of turbulent diffusion. The continual growth and trajectory of turbulent eddies in the free shear layer is no longer conserved. This trend will be confirmed later by tracking their path. The slope of the decay rate of the perturbed jet plotted in the logarithmic form is found equal to -0.45 (figure not shown here), this value is higher than that found in the case of the unperturbed jet, where the slope is found equal to -0.69. The value quoted by Schneider and Goldstein (1994) was -0.608 in the case of a non disturbed two-dimensional wall jet in stagnant surroundings. Recall that, the determination of the slope depends on the downstream location from which a linear fit should be applied. For instance, the fitting line in the case of (Eriksson *et al.*, 1998) was applied in the range between x/e = 40 and 150.

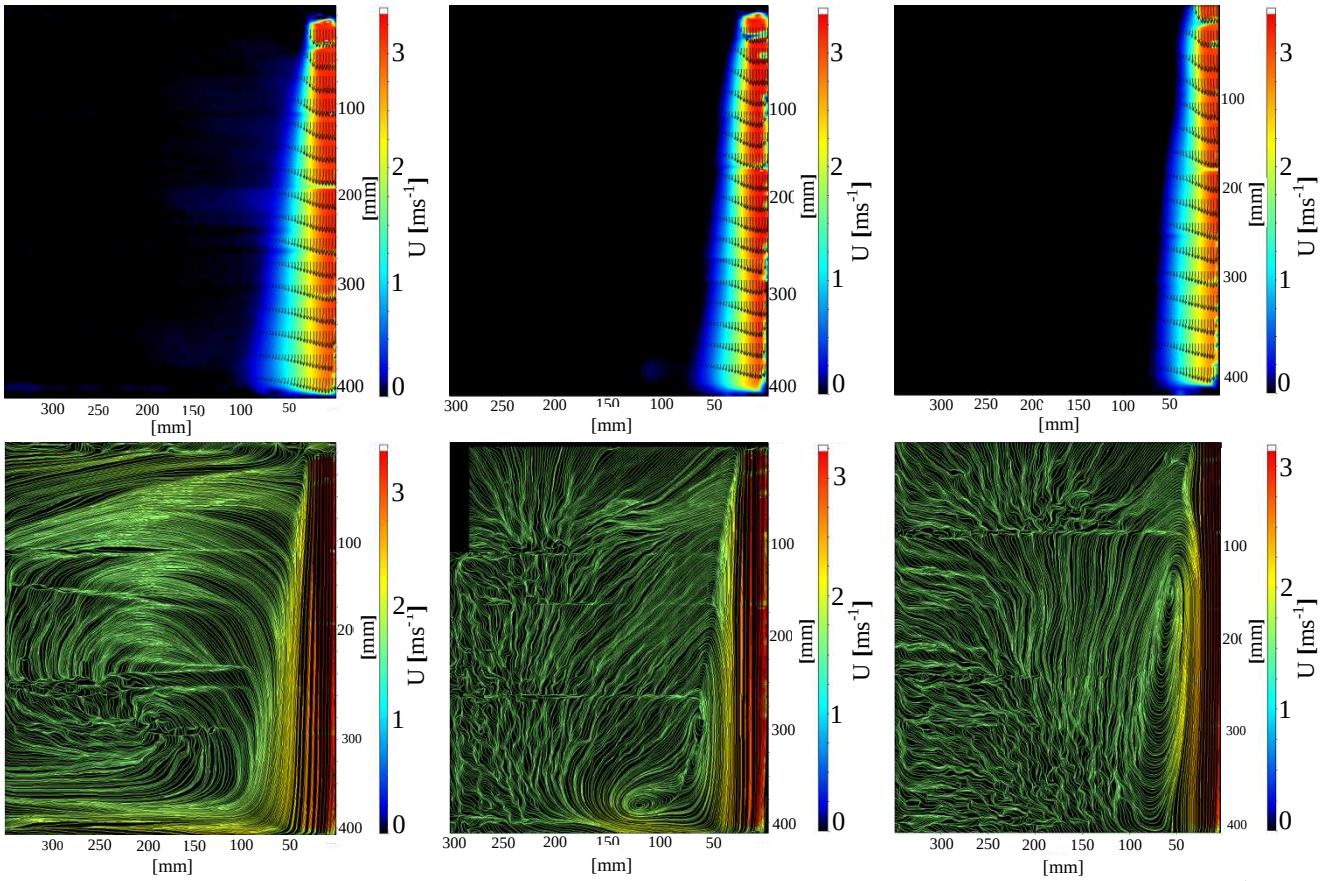

***a**. Unperturbed jet* ***b**. Perturbed jet at 0.5 m/s* ***c**. Perturbed jet at 1 ms^{-1}*

Figure 4 Velocity fields and streamlines of the perturbed and unperturbed jet at velocities 0.5 ms^{-1} and 1 ms^{-1}

4. 4 Spread rate

Figure 6 shows the evolution of the half-width growth rate of the perturbed wall jet at 1 ms^{-1}. As it can be seen, just near the nozzle exit at x/e = 2 both the unperturbed and perturbed jet have almost the same expansion value. Further downstream, values of the perturbed jet are seen to drop down. The effect of the vortex loop as previously shown in Figure 4.c developing in the shear layer of the disturbed jet is responsible of the concave curve shape between the two downstream locations x/e = 2 and x/e = 5, a plateau-like shape is noticed at streamwise positions x/e = 3 and x/e = 4. Further downstream, the curve follows the same increasing slope trend like the unperturbed jet. It seems like that the perturbed jet undergoes a phase lag due to the higher aerodynamic interaction which will be recovered further downstream for x/e > 4.

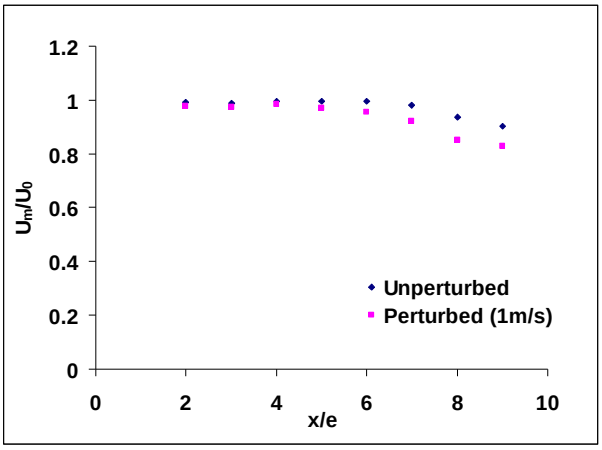

Figure 5 Decay rate of the streamwise velocity

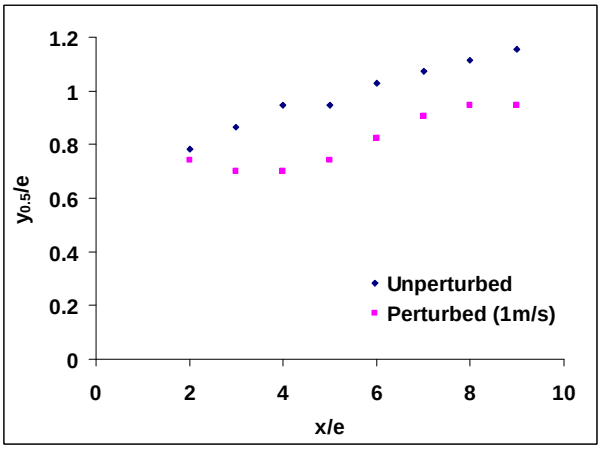

Figure 6 Half- width growth of the perturbed

Therefore, the ELS plays a retarding effect on the spread rate of the perturbed jet. As an indication to the lower lateral expansion of the perturbed jet, in the linear portion at x/e = 8, the ELS decreases the spread rate of the wall jet of about 15 %. A linear regression approximation of these two curves may be applied even though the zone where the jet is believed to attain its self-similarity is very short. For x/e > 5 a growth rate value of 0.05 is obtained which is lower than that quoted by many authors (the slope is equal to 0.07 in the case of Eriksson et *al.*, 1998). This discrepancy may be also due the configuration of the recycled wall jet.

4.5 Spectral analysis of Kelvin-Helmholtz instability

Fast Fourier Transformations (FFT) has been applied to the streamwise fluctuant velocity at downstream location x/e = 3 in the free shear layer (y/e = 1.3) in order to study the effect of the perturbing span-wise channel flow on the development of Kelvin-Helmholtz instability. The obtained spectra (Figure 7) revealed a peak frequency of 47.5 Hz in the case of undisturbed jet and 36.5 Hz and 27 Hz when disturbed laterally by the ELS jet blowing at two increasing velocities (0.5 ms^{-1} and 1 ms^{-1}). These values correspond to calculated Strouhal numbers (based on nozzle width) of 0.6, 0.45, and 0.36. The Strouhal number based on the nozzle width is defined as follows:

$$St_e = \frac{fe}{U_0} \tag{2}$$

Where $\boldsymbol{f}$ is the peak frequency, $\boldsymbol{e}$ is the nozzle width and $\boldsymbol{U_0}$ is the nozzle exit velocity. The engulfment of ambient air is significantly reduced by the ELS effect. The reduction in the shedding frequency might be explained by the break-up of the mechanism of roll-up and pairing of K-H vortices which are responsible of the large spread of air curtain. In fact, the ELS affect the topology of the K-H instability as depicted in Figure 9. K-H instability becomes deformed and elongated with the streamwise direction at U_{lf} = 0.5 ms^{-1} and detached at U_{lf} = 1 ms^{-1} due to the break-up of filaments in the braid region (region situated between two Kelvin-Helmholtz rollers). The lateral flow enables an active control of vortex formation. The evolution of Strouhal number along the jet axis for three streamwise positions x/e = 3, x/e = 5 and x/e = 7 is shown in

figure 8.As it can be seen the Strouhal number decreases with increasing downstream locations, this trend is similar to that observed in the case of unperturbed free plane jets. At U_{lf} = 0.5 ms^{-1}, the evolution is a little bit different from the two other curves since it tend to stabilize from x/e = 5. This may be due to a noisy signal which makes the differentiation of the peak a difficult task, even at a higher sampling rate, PIV technique has its drawbacks compared to single point measurement techniques. It should be noted that the spectral analysis has been performed on an area of interest of 1024×128 pixels for each streamwise position at a sampling rate of 10 kHz. In a real RDC, the Strouhal number which characterizes the vortex shedding frequency is desired to be as lesser as possible, since the entrainment of the ambient air occurs in the shearing interface where indentation and protrusion develop and contribute to the widening if the mixing layer of the air curtain.

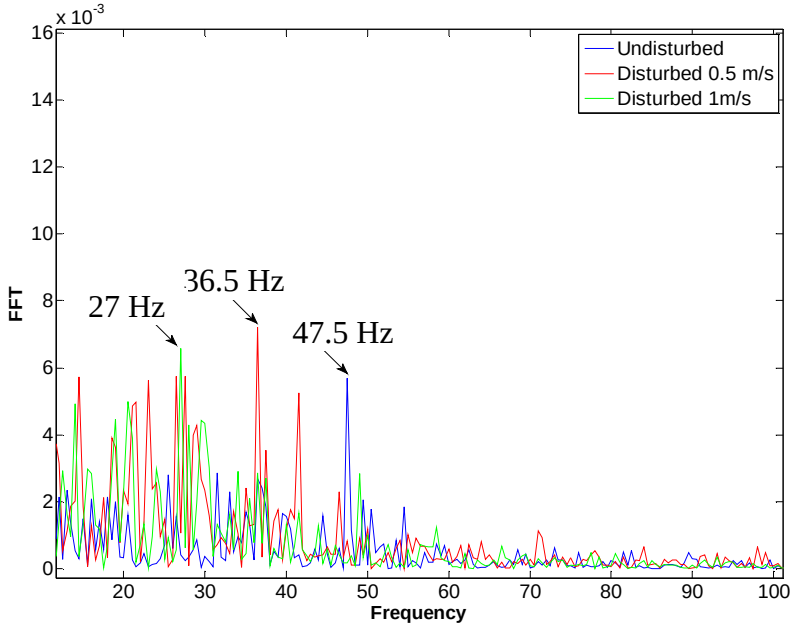

Figure 7 FFT of undisturbed and disturbed jet at x/e = 3 and y/e = 1.3

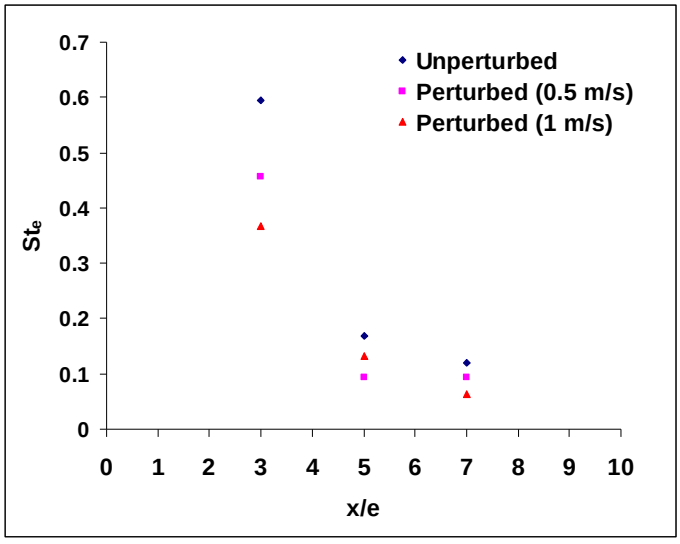

Figure 8 Streamwise evolution of Strouhal number

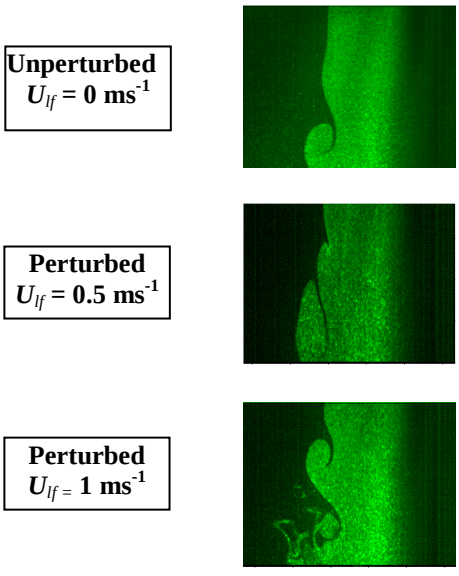

Figure 9 Kelvin Helmholtz instability topology

5 CONCLUSIONS

In this study the effect of the ELS on the wall plane jet applied to a RDC has been investigated experimentally via PIV measurements. This study has revealed that the lateral perturbation has largely affected the jet expansion leading to a significant decrease in the entrainment strength and a weakening in the mixing layer thickness. This effect is favoured especially by decreasing the amount of the ambient air entrained by the air curtain. The lateral flow also tends to move the inflection point closer to the wall. The velocity decay rate is higher in the case of the perturbed jet, hence the length of the potential core decreases. The velocity vector maps covering the whole air curtain show a recirculation loop at the lower part of bottom of the perturbation channel at a velocity of $0.5 m.s^{-1}$. Further increase in the velocity to 1 ms^{-1} leads to a displacement of the recirculation loop upstream the air curtain to be situated between x/e = 2 and x/e = 5, however its influence extends to cover the entire air curtain. It's found through a spectral analysis that the Strouhal number decreases with increasing ELS velocity. This behavior has been explained by the altered K-H instability topology which experiences a deformation at U_{lf} = 0.5 ms^{-1} and a detachment at U_{lf} = 1 ms^{-1} causing a reduction in the shedding frequency due to the break-up of the roll-up and pairing mechanism which are responsible of the large spread of air curtain.

REFERENCES

1. Gaspar P. D, Carrilho Gonçalves L.C, Pitarma R.A. 2011, Experimental analysis of the ther1mal entrainment factor of air curtains in vertical open display cabinets for different ambient air conditions. *Applied Thermal Engineering* 31: 961-969.
2. Cortella G, 2002, CFD-aided retail cabinets design. *Computers and Electronics in Agriculture* 34: 43-66.
3. Laguerre O, Hoang M.H, Osswald V, Flick D. 2012, Experimental study of heat transfer and air flow in a refrigerated display cabinet, *Journal of Food Engineering* 113: 310-321.
4. Field B.S and Loth E. 2006, Entrainment of refrigerated air curtains down a wall, *Experimental Thermal and Fluid Science*, 30 (3): 175-184.
5. Glauert M. B, 1956, The wall jet, *Journal of Fluid Mechanics* 1(6): 625-643.
6. Bradshaw P and Gee M. T, 1960, Turbulent wall-jets with and without external stream, Aeronautics Research Council Reports and Memoranda No. 3252.
7. Bajura, R. A. and Catalano, M. R. 1975, Transition in a Two-Dimensional Plane Wall Jet, *Journal of Fluid Mechanics* 70, Part 4: 773-799.
8. Hsiao FB, Sheu SS. 1996, Experimental studies on flow transition of a plane wall jet. *Aeronautical Journal* 100 (999):373-380.
9. Cao Z, Gu B, Han H, Mills G. 2010, Application of an effective strategy for optimizing the design of air curtains for open vertical refrigerated display cases. *International Journal of Thermal Sciences* 49 (6): 976-983.
10. van Hooff T, Blocken B, Defraeye T, Carmeliet J, van Heijst, G.J.F. 2012a, PIV measurements of a plane wall jet in a confined space at transitional slot Reynolds numbers. *Experiments in Fluids,* 53(2): 499-517.
11. Hunt, J.C.R., Wray, A.A., Moin, P., 1988. Eddies, stream, and convergence zones in turbulent flows. *Center for Turbulence Research Report* CTR-S88, pp. 193–208
12. Rajaratnam N. 1976, *Turbulent Jets*, Elsevier Scientific Publishing Company, Amsterdam, 303p.
13. Eriksson J.G, Karlsson R.I. and Persson J. 1998, An experimental study of a two-dimensional plane turbulent wall jet, *Experiments In Fluids* 25: 50-60.